Design of the Fast Plasma Position Control Coils for JT-60SA

Shuji ASAKAWA, Kiyoshi YOSHIDA
Japan Atomic Energy Agency, Naka, Ibaraki-ken 311-0193, Japan

(Received: 30 October 2009 / Accepted: 13 February 2010)

The upgrade of JT-60U magnet system to superconducting coils (JT-60SA) is progressing by both parties of Japanese government and European commission in the framework of the Broader Approach agreement. Two in-vessel conventional copper coils are required for the fast plasma position control. Two 4 m diameter circular coils with 120 kA supply the required magnetic field. This paper describes the technical requirements, the detailed design, and analysis results of the fast plasma position control coils for JT-60SA.

Keywords: fusion, magnet, internal coil, JT-60, broader approach

1. Introduction

The JT-60 tokamak is upgrading to an advanced superconducting tokamak JT-60SA (JT-60 Super Advanced) [1, 2], and be operated under the framework of this Agreement as a "satellite" facility for ITER. The Satellite Tokamak Programme is expected to develop operating scenarios and to address key physics issues for an efficient start up of ITER experimentation and for research towards the fusion DEMO reactor. The superconducting magnet system [3, 4] for JT-60SA consists of 18 Toroidal Field (TF) coils, a Central Solenoid (CS), six Equilibrium Field (EF) coils as shown in Fig. 1. However, JT-60SA requires two poloidal coils inside the vacuum vessel for the fast plasma position control to stabilize high elongation and triangularity of plasma.

The fast plasma position control (FPPC) coils are designed in the JT-60SA tokamak as shown in Fig. 2. Two coils provide independent control of vertical and horizontal field. Total ampere-turn of each coil is 120kA. Size of current center is 4 m in radius. The FPPC coils shall be supported by 18 points in toroidal direction from the vacuum vessel (VV).

Existing large tokamaks JET and JT-60U use the internal coils. The internal coils for JET were constructed inside the vessel [5, 6]. Internal coils for JT-60U were fabricated outside the VV and then assembled inside the VV. The internal coil for EAST [7] was also connected conductor inside VV. The Direct winding inside VV is proposed for JT-60SA.

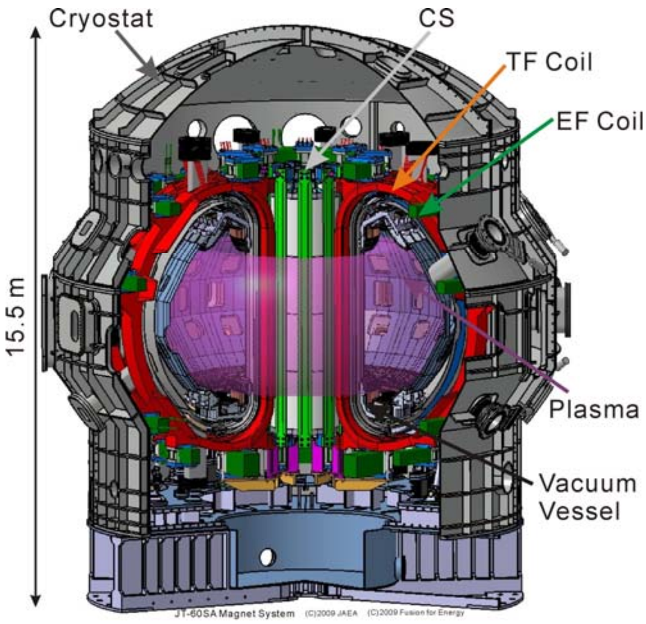

Fig. 1 JT-60SA basic device

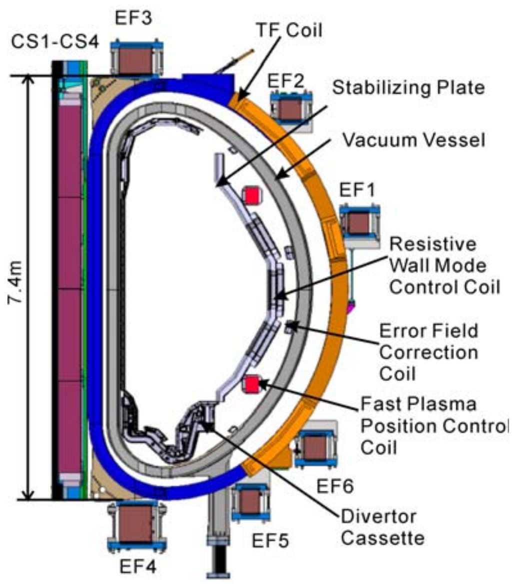

Fig. 2 Cross section of the JT-60SA

2. Requirements for the FPPC Coil

The total current of the FPPC coils is required as large as much possible to increase the plasma control performance. A total current of 120kA is selected considering the limited space inside the VV, as shown in Fig. 2, as well as the strength of the support structure. The FPPC coils are located between VV and the stabilizer plate. There are feeder conductors from the collection

author's e-mail: asakawa.shuji@jaea.go.jp

coils between the FPPC coils and VV wall.

The FPPC coils are attached to the VV wall through flexible support plates allowing radial displacements. The winding pack itself supports own hoop force and bending between supports. Operational cycles is 18,000,000 based on 10 Hz cycles during 100s operation for 18,000 of plasma operation shots. The VV is heated up 200 ºC during baking mode. The design parameters based on these specifications are shown in Table 1 and Table 2.

Radiation dose from D-D neutron emission rate 1.5 x 10^{17} (n/year) is 0.6 MGy during 10 years operation. This dose values can allow to use epoxy insulation system developed for superconducting insulation system during ITER-EDA [8].

3. Design of the FPPC Coil

3.1 Winding and Case

The Oxygen-Free Copper (OFC) conductor with the hole for water cooling is adapted for the FPPC coil. The tensile strength of half hard OFC (JIS H 3300) is more than 245 MPa. Conductor size is 31 mm square and 12 mm circular cooling hole as shown in Fig. 3. The flow speed of cooling water is 1 m/s to remove heat during 1800 s interval. Pressure drop is 0.8 MPa for 600 m cooling length with 12 mm diameter cooling hale. The cooling pass consists of single channel to avoid additional cooling pipes.

The glass-cloth epoxy can be used for the insulation system until radiation dose of 1 MGy. The turn insulation and the ground insulation of FPPC coils can use the vacuum impregnation type regin (DGEBA: diglycidyl ether of bisphenol A epoxy) or pre-impregnated type regin (TGDM: tetraglycidyl diaminodiphenyl methane) developed in ITER-EDA [8]. This glass-epoxy insulation system is similar to the EF coil. The glass-cloth for insulation shall be Boron free glass fiber as R-glass or E-glass. At least one layer of Polyimide film is recommended to avoid the dry region for the vacuum impregnation process. The spacer for casing is G10 grade FRP with same composite as turn insulation.

The winding pack consists of a hexa-pancake with one conductor without joint. The conductor has the turn insulation. Winding pack has the ground insulation. The steel case of thin plates of Inconel 625 covers the winding pack and the feeder conductor to make a separate vacuum for the winding pack. For closing weld, four surfaces of the winding pack are covered with the G10 plates. Corners of the case are filled by the glass fiber for thermal insulation during closing welding. The coil case is clamped by two flanges and two plates.

The flexible plates are connected from the clamp on the coil case to the attachment to VV as shown in Fig. 4. The support structure is designed based on the forces

Table 1 Requirements and design conditions of the FPPC coils

Items	Values
Number of coil	2
Total current (kA)	120
Mean radius of winding (m)	4
Height from the plasma center	+/- 1.6
Duration of full current (s)	100
Interval of shot (s)	1,800
Coolant	Water
Baking temperature (°C)	200
Operational Cycles	18,000,000
Radiation Dose (MGy)	0.6

Table 2 Design parameters of the FPPC coils

Items	Values
Conductor current (kA)	5.22
Number of terns	23
Mean radius of winding (m)	3.975
Height from VV center	+/- 1.665
Coolant speed (m/s)	1.0
Maximum temperature (°C)	155

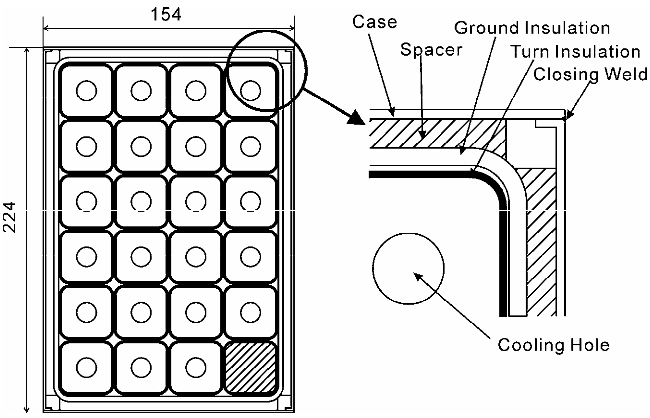

Fig. 3 Cross section of FPPC coil (mm)

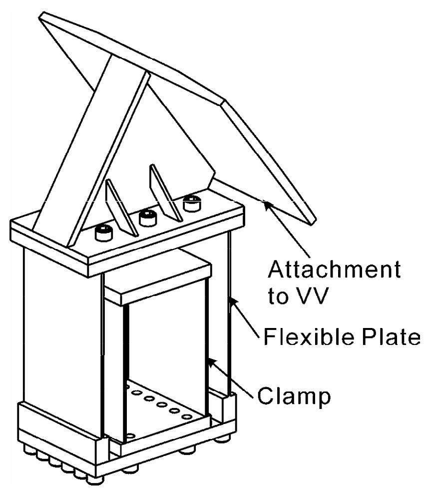

Fig. 4 Support for the FPPC coil

transmitted to, and from the VV. Then, force absorbed through bowing of the flexible plate. The support structure is expected to be a bolting tie structure which allows to the position adjustment as well as electrical insulations. The support consists of 18 sets of the coil clump and two flexible plates.

3.2 Manufacturing Process

The FPPC coils for the JT-60SA can be wound inside VV because the FPPC coil has relatively many turns (23 turns) and because the conductor can be supplied from outside through a tangential port. One long conductor (600m) can be wound in side of the VV without the basing process of copper conductor. The manufacturing period of the FPPC coils will be minimized by the direct winding inside the VV. The facilities for the fabrication of the CS and EF conductor in Naka site will be used to manufacture a spool with length of 600 m copper conductor.

The coil is wound inside the VV. The conductor wound around the spool is set up outside the VV and guided inside through the port as shown in Fig. 5. The conductor is introduced from the spool into the VV through a tangential port. The working floor is set up within the VV and the coil is formed by using a bender and a turntable. Fig. 6(a) shows the construction of the coil on the flower. Fig. 6(b) shows lifting the completed upper coil. The coil is positioned using a crane. In case of JT-60SA, EF coil manufactur in the onsite factory at Naka site. There are many tools can be reused from the EF superconducting coil fabrication in Naka site.

3.3 Feeders

Feeder from the FPPC coil to the port in the VV is shown in Fig. 7. The terminations of the conductor from winding pack are located at inner most turn by space limitation. The conductor from the winding pack is terminated at the joint box. The feeder conductor is penetrated with the radial insulation bossing at flange for the port. All feeders with case are supported from VV and port though steel plates for thermal insulation during baking mode.

4. Analysis of the FPPC Coil

4.1 Electromagnetic Force

The plasma disruption simulation with DINA code [9] is carried out to calculate the electromagnetic force of the FPPC coils. The DINA code calculates free boundary plasma equilibria, taking into account eddy currents in the VV and a model of the power supplies. The downward VDE disruption, upward VDE disruption and major disruption (MD) in center are evaluated by the simulation.

The VDE is caused by vertical instability due to loss of control. The VDE simulation is performed by following conditions:

(1) Disruption (thermal quench) starts at qedge=1.5,

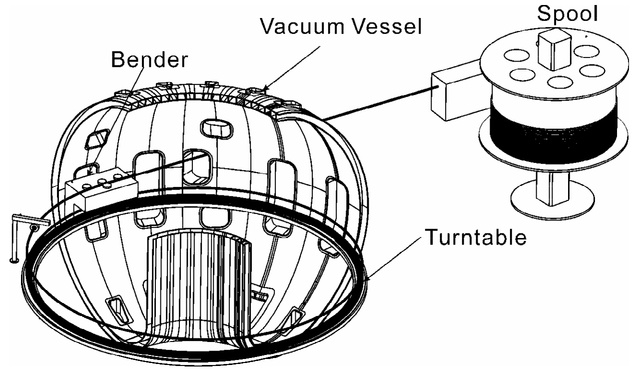

Fig. 5 Winding the coil inside vacuum vessel

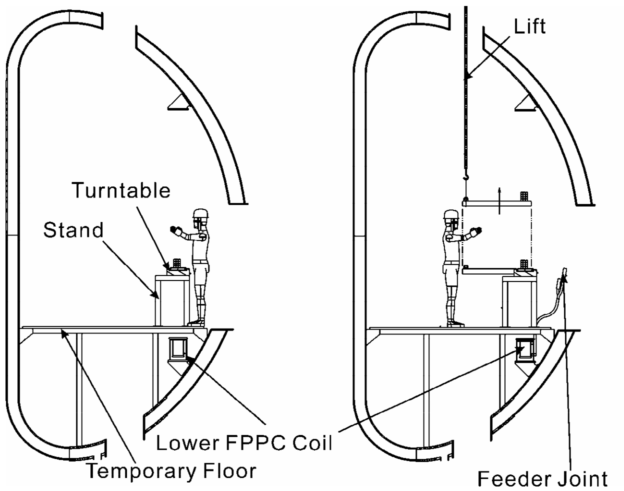

(a) Winding (b) Lift the upper coil

Fig. 6 Coil manufacturing cross section

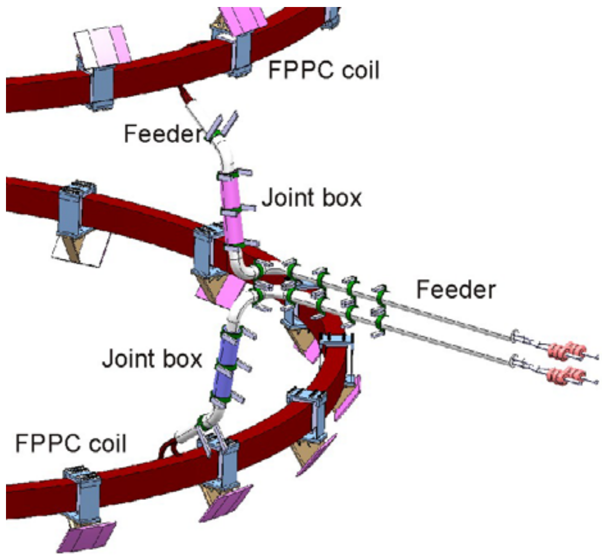

Fig. 7 Feeder for the FPPC coil

(2) 0.5 ms after thermal quench, current quench starts,
(3) Plasma Current decreases linearly in 10 ms and 30 ms.

As for MD, Plasma stays at center when disruption (thermal quench) starts. The MD simulation is carried out by following assumptions:
(1) Current quench starts 0.5 ms after thermal quench,
(2) Plasma Current decreases linearly in 4 ms.

The VV and the stabilizing plate in JT-60SA are modeled for the DINA simulation. The DINA disruption simulation incorporates a detailed axisymmetric representation of the VV and in-vessel systems. The VV and stabilizing plate is modeled by a set of thin plates with relevant resistance, so that the global L/R time can be matched with that calculated for the actual geometry. The VV consists of SS316L double wall with 18mm thickness and is modeled to separate 112 toroidal passive plates. The stabilizing plate consists of SS316L double wall with 10mm thickness and is modeled to separate 66 toroidal passive plates. As for boundary, coordinates of the plasma facing line are determined as a limiter of plasma by the first wall and the divertor. As for PF coils, CS2 and CS3 are series-connected. For the initial plasma for DINA simulation, the plasma equilibrium at end of burn with the maximum current 5.5MA and typical other parameters are shown in Table 3.

The FPPC coils are supposed to be short-circuited in case of MD. The maximum rated value ±5 kA is added as initial current to FPPC coils current. The largest absolute values for the electromagnetic force of the inward and outward radial electromagnetic force are shown in Table 4.

4.2 Thermal Analysis

The coil and the 18 support structures supporting the coil are modeled for the thermal analysis (during baking mode) and stress analysis using ANSYS [10]. The analysis region is 1/36 model that considers symmetry. The analytical model approximates the conductor (copper), insulation material, case and coil support structures. The support structures are formed of flexible plates both side of the coil. Fig. 8 shows the coil and support structures for the analysis model.

Normal operation mode, outlet temperature of conductor during 100s operation is shown in Fig.9. The temperature in the cooling water is less than 63 °C because resistive heat generation is relatively low during 100 s.

During baking operation mode, the vacuum vessel and ports are heated up to 200 °C. The winding pack is cooled by water. Supply temperature of cooling water is 42 °C. Radiation is considered from all surface to the case and support structures. The emissivity of the case is 0.7 as same as normal steel. The contact surface with the VV is specified at 200 °C. However, the temperature

Table 3 Plasma parameters for the DINA simulation

Items	Symbol	Values
Plasma current (MA)	I_p	5.5
Poloidal beta	β_p	0.83
Internal inductance	l_i	0.71
Elongation	κ	1.86
Plasma minor radius (m)	a	1.14
Mean radius of winding (m)	R_{cur}	2.97
Winding height (m)	Z_{cur}	0.034
Safety factor	q_{95}	2.70
Electron temperature (keV)	T_e	9.1
Effective ion charge	Z_{eff}	2.0
Plasma density (m^{-3})	n_e	5×10^{19}

Table 4 Electromagnetic force by the DINA simulation

Case (MN)	Vertical direction	Radial direction
VDE DW 30ms	-1.93	4.05
MD 4ms	1.54	-6.14

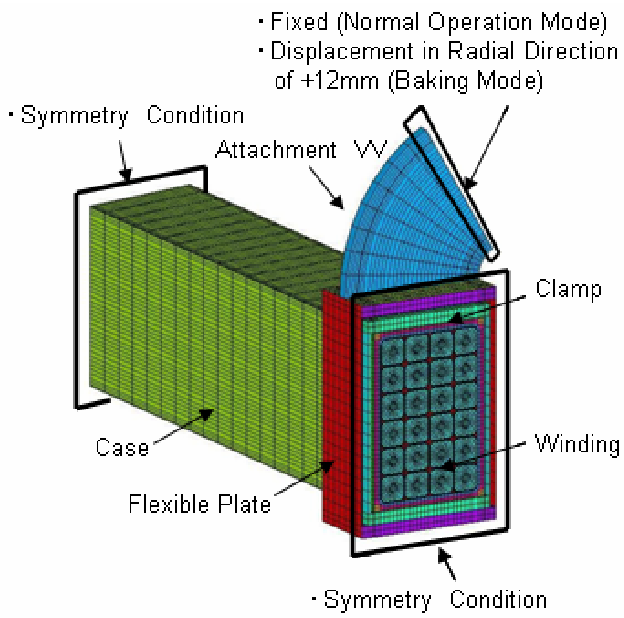

Fig. 8 Analysis model and mechanical boundary conditions

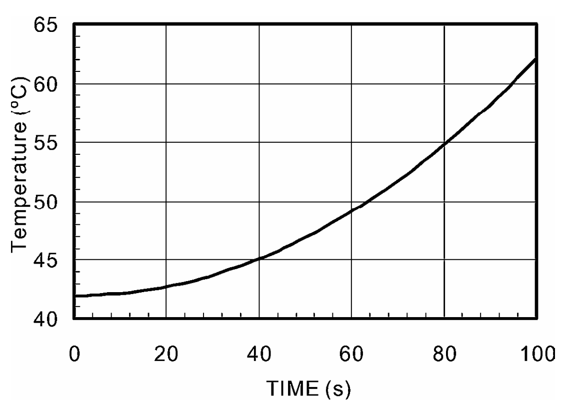

Fig. 9 Outlet temperature during normal operation

decreases at the flexible plates. Fig. 10 shows temperature distribution during baking mode. The flexible plate has a good thermal resistance to reduce heat to the winding pack. The temperature of the winding pack is less than 83ºC at baking mode. The insulation made by the glass-epoxy can be feasible during baking mode and normal operation mode.

4.3 Mechanical Analysis

As boundary condition, symmetry conditions are imposed on the circumferential symmetry plane. The surface in contact with the VV is a fixed boundary in normal operation mode. In baking mode, the surface in contact with the VV is displaced by +12mm in the radial direction. Fig. 8 shows the mechanical boundary conditions.

All cases, the thermal load (temperature distribution) is given, respectively, and electromagnetic force in the radial and vertical directions is given on the conductor for normal operation mode. The analytical cases have electromagnetic force acting on cases VDE DW 30ms and MD 4ms.

The maximum tresca stress of the conductor, the case and the flexible plate is 32, 325 and 405 MPa, respectively. These stresses are much less than limit of stress intensity. The maximum shear stress of the insulation is 9.9 MPa that is less than limit of share stress (27 MPa) on the insulation material. Fig. 11 and Fig. 12 show the tresca stress distribution at the MD 4ms and baking mode condition of the conductor and support structure, respectively. The stress evaluation results for the conductor and flexible plate meet the design standard [11]. Table 5 and Table 6 show the stress evaluation result for the conductor and the flexible plate, respectively.

Table 5 Stress evaluation of the copper conductor

(MPa)	Membrane stress	Membrane + Bending stress	First + secondary stress	First + Secondary + Peak stress
Limit of stress intensity	Sm	1.5Sm	3Sm	2Sa
	81.7	122.6	245.1	-
VDE DW 30ms	17.2	18.7	22.6	27.2
MD 4ms	14.1	15.3	27.7	31.3
Baking mode	-	-	27.5	32.0

Table 6 Stress evaluation of the flexible plate (Inconel 625)

(MPa)	Membrane stress	Membrane + Bending stress	First + secondary stress
Limit of stress intensity	Sm	1.5Sm	3Sm
	276	414	828
VDE DW 30ms	29.8	37.7	147.5
MD 4ms	30.1	56.9	132.6
Baking mode	-	-	405.1

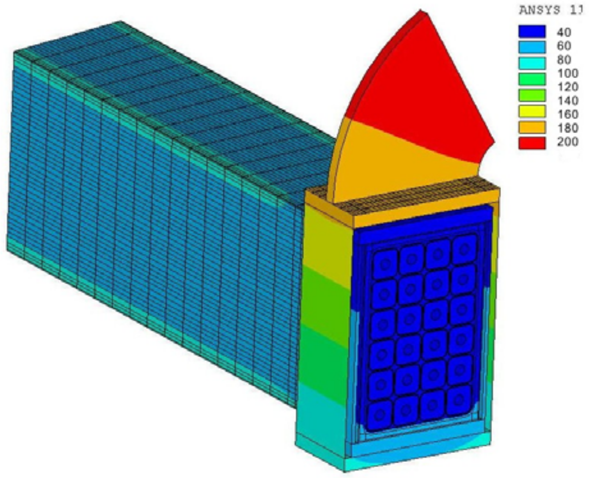

Fig. 10 Temperature distribution at baking mode (℃)

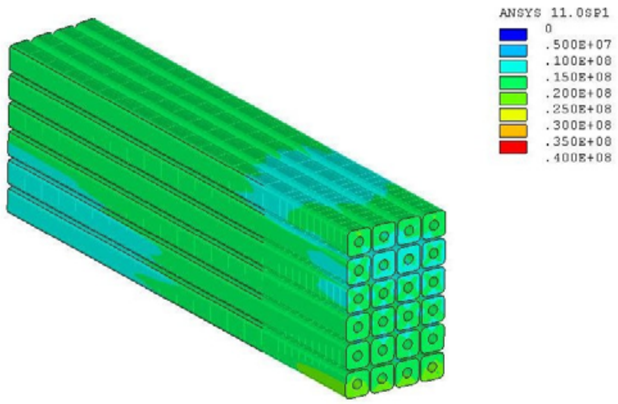

Fig. 11 Tresca stress distribution in the conductor at MD 4ms (Pa)

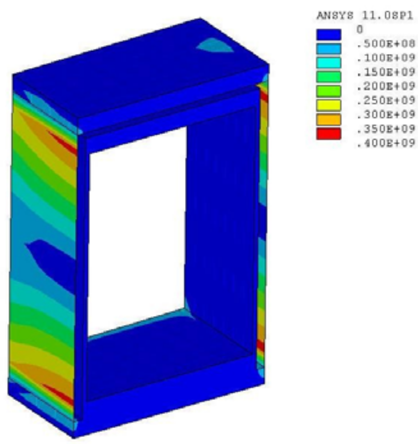

Fig. 12 Tresca stress distribution in the support structure at baking mode (Pa)

5. Conclusions

This report presents the design, the manufacturing and the analysis for the FPPC coils for JT-60SA. Two

120kA FPPC coils can be designed to satisfy the design criteria in both the maximum temperature and mechanical strength. The glass-epoxy insulation system can be applied for the FPPC coils as similar as the EF superconducting coil. The direct winding inside the VV is the candidate manufacturing process to minimize the manufacturing period of two FPPC coils. Many conductor fabrication tools and EF coil fabrication tools can be reused for the fabrication of the FPPC coils in Naka site.

Acknowledgments

The authors would like to thank Dr. M. Takechi of JAEA for his plasma analysis of this study.

References

[1] S. Ishida, P. Barabaschi, Y. Kamada, "Status and Prospect of the JT-60SA Project ", in 9th International Symposium on Fusion Nuclear Technology (ISFNT-9), Oct. 11-16, 2009 in Dalian, China, to be published.

[2] Y. Kamada, S. Ishida, P. Barabaschi, "Progress of JT-60SA project towards an integrated research for ITER and DEMO", in the Asia Plasma and Fusion Association (APFA2009), October 27-30 2009, Aomori, Japan,, to be published.

[3] K. Yoshida, K. Tsuchiya, K. Kizu, et al., "Design and Construction of JT-60SA Superconducting Magnet System", in the Asia Plasma and Fusion Association (APFA2009), October 27-30 2009, Aomori, Japan, to be published.

[4] K. Tsuchiya, K. Kizu, H. Murakami, et al., "Recent progress of the design activity for the poloidal field coil system in JT-60SA", in 21st International Conference on Magnet Technology (MT-21), 18-23 October 2009, Hefei, Anhui, China, to be published.

[5] E. Bertolini, G. Celentano, J. R. Last, et al., "The Jet Divertar Coils", IEEE TRANSACTION ON MAGNETICS, 28, 1 (1992) 275-278.

[6] N. Dolgetta, E. Bertolini, C. D'Urzo, et al., "JET Divertor Coils, Manufacture, Assembly and Testing", IEEE TRANSACTION ON MAGNETICS, 30, 4 (1994) 2150-2153.

[7] Shijun Du, Xufeng Liu, "Design and fabrication of the active feedback control coils for EAST", Fusion Engineering and Design, 83 (2008) 766-770

[8] P. Rosenkranz, K. Humer, H. W. Weber, et al., "Irradiation effects on the fatigue behaviour of an ITER candidate magnet insulation material in tension and interlaminar shear", Fusion Engineering and Design, 58-59 (2001) 289-293

[9] R. R. Khayrutdinov, V. E. Lukash, "Studies of Plasma Equilibrium and Transport in a Tokamak Fusion Device with the Inverse-Variable Technique", JOURNAL OF COMPUTATIONAL PHYSICS, 109 (1993) 193-201

[10] ANSYS Inc. ANSYS Multiphysics (2009)

[11] JAME, "Codes for Fusion Facilities - Rules on Superconducting Magnet Structure -", JSME S KA1-2008 (2008)